

# Letters

---

## Ultrathin Au Electrodes Based on a Hybrid Nucleation Layer for Flexible Organic Light-Emitting Devices

Yan-Gang Bi, Fang-Shun Yi, Jin-Hai Ji, Chi Ma, Wen-Quan Wang, Jing Feng, and Hong-Bo Sun<sup>✉</sup>, Fellow, IEEE

**Abstract**—We report an ultrathin Au transparent electrode with the thickness of only 4.4 nm based on an S-1805/Ag hybrid nucleation layer and its application in flexible organic light-emitting devices (OLEDs) as the replacement of indium tin oxide (ITO) anode. The Volmer–Weber growth mode of the deposited Au film has been suppressed successfully by using the hybrid nucleation layer, in which the S-1805 acts as a substrate modification layer and 0.6 nm Ag acts as a seeding layer. The resulting ultrathin Au film with the thickness of 4.4 nm shows high transparency, high conductivity, and ultrasmooth surface. A 25% improvement in efficiency has been demonstrated for the OLEDs with ultrathin Au anodes compared to the ITO-based devices. The application of the high-performance ultrathin Au electrodes in OLEDs results in high flexibility and mechanical robustness with small performance variations after 2100 bending cycles with a 7.5 mm bending radius.

**Index Terms**—Transparent electrodes, ultrathin metal film, hybrid nucleation layer, organic light-emitting devices.

### I. INTRODUCTION

DURING the last decades, extensive attention has been paid to transparent conducting electrodes owing to their widespread applications, including transparent display devices, touch screen panels, organic optoelectronic devices, and transparent film heaters [1]–[5]. With high conductivity and transmittance, indium tin oxide (ITO) has been considered as the

most traditionally used transparent conductive electrode (TCE) [6], [7]. However, ITO suffers from the increasing price with limited indium resource, insufficient conductance for large-area devices, and incompatibility with flexible devices due to its poor flexibility and high annealing temperature during fabrication [8]–[10]. To break through the limitations of ITO, a series of novel TCEs have been developed, such as metal nanowires [11], carbon nanotubes [12], [13], graphene [14]–[16], conductive polymers [17], patterned metal nanostructure grids [18]–[20], and ultrathin metal films [21]–[24]. Despite of the flexibility of carbon-based materials and conductive polymers, the low conductivity limits their applications as electrodes [25], [26]. Metal nanowires and patterned metal nanostructure grids need complex synthetic and fabrication processing, which restricts the electronic performance of organic optoelectronic devices [27], [28].

A continuous and transparent ultrathin metal film with low electrical resistivity and high flexibility has been considered as a promising replacement of ITO [29]. Unfortunately, it is well known that the thermally evaporated or sputtered ultrathin metal film (<10 nm) follows the Volmer–Weber growth mode usually exhibiting a discrete granular and rough morphology due to the bad adhesion with the substrate, which largely decreases the optical transparency and deteriorates their electrical conductivity [30]. A possible solution is to introduce the “adhesive layer” to reinforce metal nucleation by physisorption [31] or chemisorption [32], such as metal [33], [34], metal oxide [35], [36], and organic molecule [37]. However, the thickness of ultrathin metal film still limits the transmittance due to the requirement of desired conductivity. Up to now, it is still highly desirable to achieve an ultrathin, continuous, conductive, transparent and mechanically flexible metal film by a simple and low-temperature process with a low cost.

In the paper, we demonstrate an ultrasmooth and ultrathin Au transparent film with the thickness of only 4.4 nm based on a hybrid nucleation layer fabricated by a low-cost and simple method. The hybrid nucleation layer, which consists of a S-1805 film as the substrate-modification-layer and 0.6 nm Ag film as the seeding-layer, successfully suppresses the Volmer–Weber growth mode induced three-dimensional (3-D) islands formation of the ultrathin Au film. Based on the combined effects of Ag wetting behavior and chemical bonding between S-1805 and Au atoms, the 4.4 nm ultrathin Au film with the structure

Manuscript received April 29, 2018; revised June 15, 2018 and July 11, 2018; accepted July 23, 2018. Date of publication July 26, 2018; date of current version September 6, 2018. This work was supported in part by the National Key Research and Development Program of China under Grant 2017YFB0404501, in part by the National Nature Science Foundation of China under Grants 61675085, 61705075, 61505065, and 61605056, and in part by the China Postdoctoral Science Foundation under Grant 2016M600230. The review of this letter was arranged by Associate Editor G.-B. Lee. (*Corresponding authors:* Jing Feng; Hong-Bo Sun.)

Y.-G. Bi, F.-S. Yi, J.-H. Ji, C. Ma, and J. Feng are with the State Key Lab of Integrated Optoelectronics, College of Electronic Science and Engineering, Jilin University, Changchun 130012, China (e-mail: yangang.bi@jlu.edu.cn; 2293712485@qq.com; 503188266@qq.com; 15560291715@163.com; jingfeng@jlu.edu.cn).

W.-Q. Wang is with the College of Physics, Jilin University, Changchun 130012, China (e-mail: wangwq@jlu.edu.cn).

H.-B. Sun is with the State Key Lab of Integrated Optoelectronics, College of Electronic Science and Engineering, Jilin University, Changchun 130012, China, and also with the State Key Lab of Precision Measurement Technology and Instruments, Department of Precision Instrument, Tsinghua University, Beijing 100084, China (e-mail: hbsun@jlu.edu.cn).

This letter has supplementary downloadable material available at <http://ieeexplore.ieee.org>.

Digital Object Identifier 10.1109/TNANO.2018.2860055

of S-1805/Ag (0.6 nm) /Au (4.4 nm) exhibits extremely good surface morphology and photoelectric properties. Its root-mean-square (RMS) roughness is 0.365 nm, transparency at 550 nm is about 78.4%, and sheet resistance ( $R_s$ ) is  $70.4 \Omega \text{ sq}^{-1}$ . We have applied the ultrasmooth and ultrathin Au films with only 4.4 nm thickness in organic light-emitting devices (OLEDs) as the transparent anode to replace ITO, and a 25% enhanced current efficiency in OLEDs has been achieved compared to the devices with traditional ITO anodes. Flexible OLEDs with ultrathin Au anodes also show superior flexibility and mechanical robustness during the bending texts.

## II. EXPERIMENT

### A. Fabrication of Ultrathin Au Transparent Electrodes

The structure of the ultrathin Au transparent electrode with the hybrid nucleation layer is S-1805/Ag/Au. The glass substrates ( $20 \text{ mm} \times 18 \text{ mm}$ ) were ultrasonically cleaned by acetone, ethanol, and ultrapure water, respectively, and then dried in an oven at  $95^\circ\text{C}$  for 5 min. The diluted S-1805 (Rohm and Haas Electronic Materials, LLC) solution was spin-coated for 30 s at 3000 rpm on substrates. Then the substrates covered with S-1805 film were deal with ultraviolet (UV) exposure for 4 min. After that, the Ag seeding-layer and Au film were deposited in sequence on the S-1805 modified glass substrates.

### B. Fabrication of Flexible Au Electrodes and OLEDs

The pre-cleaned Si substrate was dealt with Octadecyltrichlorosilane (OTS) solution for about 8 h by a vapor-modification method to attain a hydrophobic surface [38]. A droplet of NOA-63 (Norland Products, Inc.) was spin-coated and then it was UV solidified for 4 min. After fabricating the ultrathin Au electrodes with the hybrid nucleation layer as well as OLEDs on the solidified photoresist films, the NOA-63 film with devices was peeled off totally from Si. The NOA-63 film with the thickness of  $50 \mu\text{m}$  acted as the flexible substrate directly. The structure of the OLEDs is substrate/TCE/MoO<sub>3</sub>/NPB/mCP:Ir(ppy)<sub>3</sub>/TPBi/Ca/Ag, and the fabrication process and characterizations of OLEDs have been reported in our previous work [9].

## III. RESULTS AND DISCUSSIONS

The Volmer-Weber growth mode can be observed obviously in Fig. 1(a). Au atoms tend to slide and gather on the surface of glass substrate due to the mismatch of surface energy, leading to the rough and discontinuous films in large region [39], [40]. The RMS roughness of the 5 nm Au film on the glass substrate is about 1.19 nm. By introducing a S-1805/Ag hybrid nucleation film, the surface morphology of discontinuous ultrathin Au film can be effectively improved. The surface morphologies of the S-1805 film and glass substrate have also been investigated in Fig. S1, which show extremely smooth surfaces and similar roughness. Fig. 1 and Fig. S2 compare the surface morphologies of thermally deposited ultrathin Au films on glass and modified substrates based on the structures of glass/Au (5 nm) and S-1805/Ag (0.6 nm)/Au (4.4 nm), respectively. The ultrathin Au

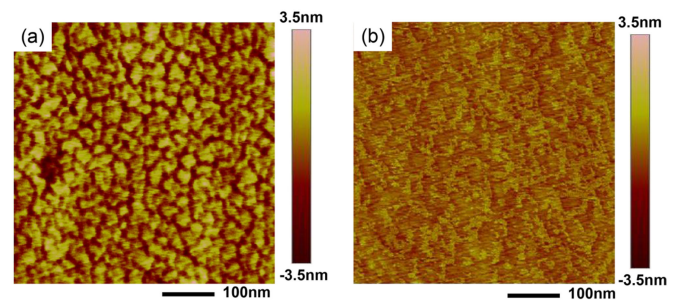


Fig. 1. AFM images of surface morphologies of (a) 5 nm Au film deposited directly on the glass substrate with the structure of glass/Au (5 nm), and (b) 4.4 nm Au film based on the hybrid nucleation layer with the structure of S-1805/Ag (0.6 nm)/Au (4.4 nm).

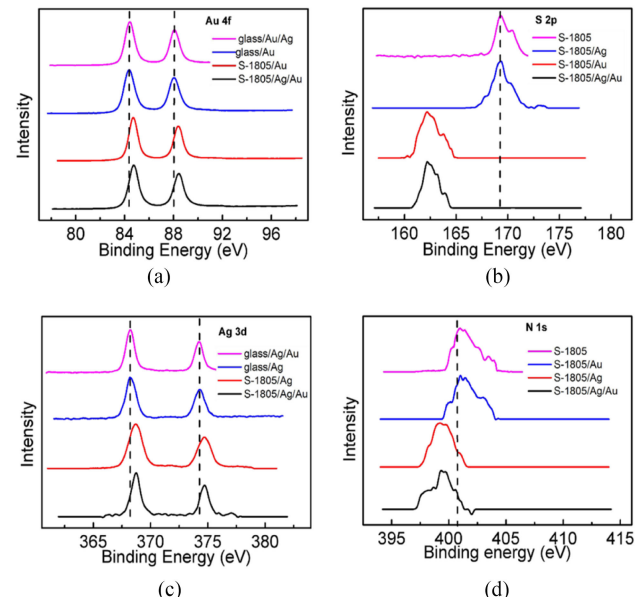


Fig. 2. XPS spectra at Au 4f (a), S 2p (b), Ag 3d (c), N 1s (d) core level of the glass/S-1805, glass/Ag, glass/Au, glass/Ag/Au, S-1805/Ag, S-1805/Au, and S-1805/Ag/Au film, respectively.

film based on the hybrid nucleation layer with S-1805 substrate-modification-layer and 0.6 nm Ag seeding-layer shows the most continuous, homogeneous and smooth surface morphology. The S-1805/Ag (0.6 nm)/Au (4.4 nm) film exhibits the RMS roughness of 0.365 nm. The improved surface morphologies based on S-1805, Ag seeding-layer, and the hybrid nucleation layer can be clearly observed by the SEM measurements in Fig. S3, respectively.

To explore the function of the hybrid nucleation layer on the growth process of metal films, we have studied the X-ray photoelectron spectroscopy (XPS) spectra of the samples with the structure of glass/Ag, glass/Au, glass/Ag/Au, glass/S-1805, S-1805/Ag, S-1805/Au, and S-1805/Ag/Au in Fig. 2 and Fig. S4, respectively. The Au 4f spectra of S-1805/Ag/Au and S-1805/Au show a chemical red shift compared to the spectra of glass/Au and glass/Ag/Au, and the S 2p spectra accordingly exhibit a blue shift compared to those of glass/S-1805 and S-1805/Ag in Fig. 2(a) and 2(b). Additionally, the XPS spectra of S-1805/Ag/Au and S-1805/Ag samples also emerge a chem-

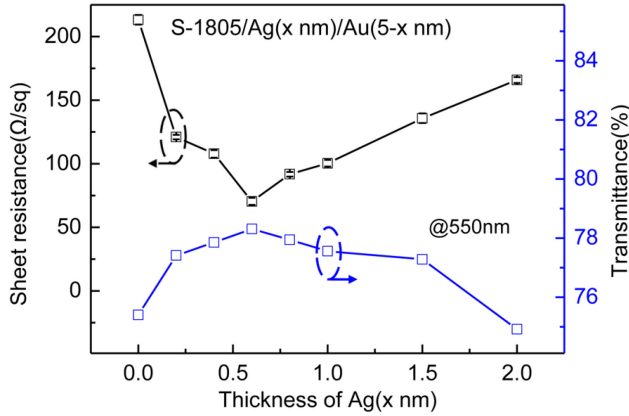


Fig. 3. Rs of the S-1805/Ag/Au film as the function of the Ag film thickness and their transmittance at 550 nm.

ical red shift at Ag 3d and a relative blue shift at the N 1s compared with control samples of glass/Ag, glass/Ag/Au, and glass/S-1805, respectively, in Fig. 2(c) and 2(d). The C 1s and O 1s spectra of all samples stay the same in Fig. S4. These chemical shifts indicate that the functional sulfur-containing and nitrogenous groups of S-1805 offer chemical bonding with Au and Ag atoms, respectively, which provide dense nucleation centers for the following deposited metal atoms [41]. On the other hand, owing to the lower surface energy of glass substrate ( $\gamma = 0.605 \text{ J m}^{-2}$ ) compared with Au ( $\gamma = 1.5 \text{ J m}^{-2}$ ), the origin of Au atoms turn to grow as isolated islands and form unconnected film on glass [42]. The Ag interlayer with  $\gamma = 1.25 \text{ J m}^{-2}$  reduces the surface energy mismatch with increased wetting behavior [43]. Based on the combined effects of Ag wetting behavior and chemical bonding between S-1805 and metal atoms, the ultrathin Au film grows uniformly and forms the ultrasmooth and continuous surface morphology.

Conductivity and transparency are crucial elements to judge the properties of transparent electrodes, and Rs is also a key indicator of continuity of ultrathin metal film. Table S1 summarizes the Rs of ultrathin Au films with various Au film thickness. A 5 nm Au film on the bare glass substrate directly is not electrically connected, while the S1805/Au (5 nm) exhibits an average Rs of  $213.2 \Omega \text{ sq}^{-1}$  due to the function of S-1805 surface-modification-layer. The conductivity of ultrathin Au film is further improved by introducing Ag-seeding-layer. The Rs of the S-1805/Ag (1 nm)/Au (2 nm) is about  $5.487 \text{ k}\Omega \text{ sq}^{-1}$ , and its conductivity rapidly increases with increasing the thickness of Au. The S-1805/Ag (1 nm)/Au (4 nm) film has a relative high conductivity with  $\text{Rs} = 100.4 \Omega \text{ sq}^{-1}$ . The transparency of Au film with structures of glass/Ag/Au and S-1805/Ag/Au have been measured as shown in Fig. S5. With the introduction of S-1805, the transparency of the ultrathin Au films is increased due to the lowered plasmon absorption, which is caused by the 3-D granular morphology of the metal film. We have further optimized the thickness of the Ag seeding layer. Rs and transparency of ultrathin Au film with various thickness of seeding layer are summarized in Fig. 3 which was collected from Table S2 and Fig. S6, respectively. With increasing the thickness of Ag, Rs of ultrathin Au film based on the hybrid nucleation

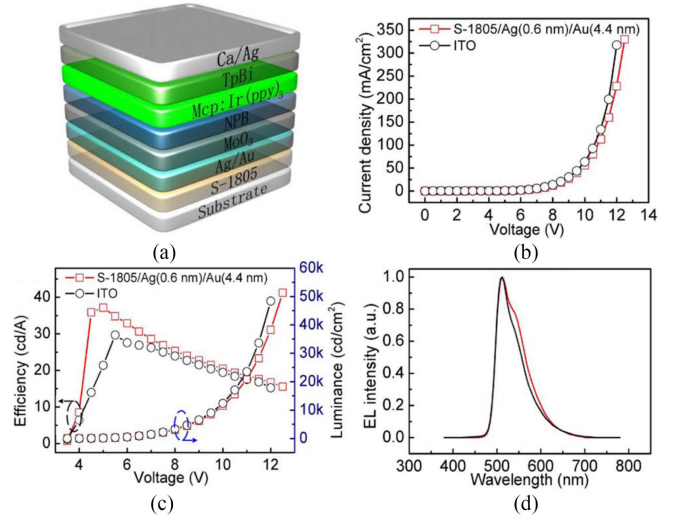


Fig. 4. EL performance of the OLEDs. (a) The schematic structure of OLEDs. Luminance-current density-voltage (b), efficiency-voltage (c), and EL spectra (d) of the OLEDs with S-1805/Ag/Au anode or ITO anode, respectively.

layer accordingly decreases until the Ag-seeding-layer exceeds 0.6 nm. The S-1805/Ag (0.6 nm)/Au (4.4 nm) film with the optimized Rs of  $70.4 \Omega \text{ sq}^{-1}$  also shows a relative high transparency of 78.4% at 550 nm, corresponding to a figure of merit of  $0.06 \Omega^{-1}$  [44], [45]. We have compared the optoelectronic properties of the ultrathin Au film with the performance of the state-of-the-art transparent conductive films in Table S3.

The undesirable thermal stability of ultrathin metal films is a serious challenge for their further applications, owing to the dewetting behavior with reconstruction of metal islands after high temperature annealing process. We have compared the normalized Rs of the 4.4 nm ultrathin Au films under various annealing temperatures and times as shown in Fig. S7, which demonstrate superior thermal stability arising from the enhanced interaction between Au atoms and the hybrid nucleation layer. The increased conductivity in the initial annealing process is induced by the improved grain boundaries of the ultrathin Au film.

The 4.4 nm ultrathin Au film based on the hybrid nucleation layer has been applied as the transparent anode in OLEDs. OLEDs with ITO anodes have also been prepared as reference. The EL properties of OLEDs are concluded in Fig. 4. Despite the slightly lower transparency of ultrathin Au film compared with ITO as shown in Fig. S8, the luminance of OLEDs is improved from  $48390 \text{ cd m}^{-2}$  to  $51330 \text{ cd m}^{-2}$  by using the ultrathin Au film as the replacement of ITO, and the current efficiency is also increased from 29.7 to 37.17  $\text{cd A}^{-1}$  with the 25% enhancement accordingly. The EL spectra of OLEDs with two kinds of anodes are almost identical (Fig. 4(d)) without obvious shifting and narrowing induced by the ultrathin Au anode. The improved EL performance of the OLEDs based on ultrathin Au anodes not only results from the excellent properties of the hybrid film but also the lessened power loss in waveguide modes due to the ITO anode with high refractive index.

To investigate the mechanical performance of the Au transparent film, the 4.4 nm flexible ultrathin Au film based on the

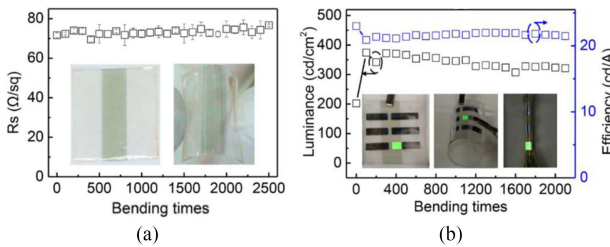


Fig. 5. Bending measurements of the 4.4 nm flexible ultrathin Au film and OLEDs. (a)  $R_s$  of the 4.4 nm flexible ultrathin Au film with different bending times. (b) Variation trend of luminance and efficiency of the OLEDs at 5 V during the bending tests. The insets show the photos of bending Au electrodes and OLEDs.

hybrid nucleation layer has been fabricated on the flexible NOA-63 substrate, and bending tests have been applied. The  $R_s$  of the ultrathin Au electrode almost remains constant after up to 2500 bending cycles with a 7.5 mm bending radius in Fig. 5(a), which demonstrates its excellent flexibility and robust mechanical capacity. In addition, there is no obvious deterioration on the EL performance (Fig. 5(b)) of the flexible OLEDs after 2100 bending cycles, and the flexible OLEDs keep stable working without dark spots or cracks after bending and even folding. The bending tests demonstrate the highly mechanical robustness and flexibility of the ultrathin Au films and ultrathin-Au-anode based OLEDs.

#### IV. CONCLUSION

In summary, we have prepared a 4.4 nm ultrathin Au film based on hybrid nucleation layer with the construction of S-1805/Ag/Au. The Volmer-Weber growth mode of deposited Au film has been suppressed effectively by the wetting behavior of Ag seeding-layer and the chemical bonding effect of S-1805 substrate-modification-layer. The 4.4 nm Au film has been applied in flexible OLEDs as the replacement of ITO transparent electrode. Due to the perfect photoelectric characteristics and advanced photon management of the ultrathin Au films, ultrathin-Au-anode-based OLEDs achieve a high efficiency with 25% improvement compared to the ITO-based OLEDs. The ultrathin Au film and OLEDs also exhibit high flexibility and robust mechanical capacity in the bending tests with small performance variations after 2100 bending cycles. This study has demonstrated that the ultrathin and ultrasmooth Au film based on a hybrid nucleation layer could satisfy the requirements of desirable TCE with high transmission, good conductivity, mechanical flexibility, and low costs in the application of wearable optoelectronic devices.

#### REFERENCES

- [1] T. Sannicolo, M. Lagrange, A. Cabos, C. Celle, J. P. Simonato, and D. Bellet, "Metallic nanowire-based transparent electrodes for next generation flexible devices: A review," *Small*, vol. 12, no. 44, pp. 6052–6075, 2016.
- [2] W. Guo, Z. Xu, F. Zhang, S. Xie, H. Xu, and X. Y. Liu, "Recent development of transparent conducting oxide-free flexible thin-film solar cells," *Adv. Funct. Mater.*, vol. 26, no. 48, pp. 8855–8884, 2016.
- [3] S. Krotkus, D. Kasemann, S. Lenk, K. Leo, and S. Reineke, "Adjustable white-light emission from a photo-structured micro-OLED array," *Light Sci. Appl.*, vol. 5, 2016, Art. no. e16121.
- [4] M. Hyunjin, W. Phillip, L. Jinwan, and K. S. Hwan, "Low-haze, annealing-free, very long Ag nanowire synthesis and its application in a flexible transparent touch panel," *Nanotechnology*, vol. 27, no. 29, 2016, Art. no. 295201.
- [5] Y.-C. Zhao, W.-K. Zhou, X. Zhou, K.-H. Liu, D.-P. Yu, and Q. Zhao, "Quantification of light-enhanced ionic transport in lead iodide perovskite thin films and its solar cell applications," *Light Sci. Appl.*, vol. 6, 2017, Art. no. e16243.
- [6] X. Li, F. Xie, S. Zhang, J. Hou, and W. C. H. Choy, "MoO<sub>x</sub> and V<sub>2</sub>O<sub>x</sub> as hole and electron transport layers through functionalized intercalation in normal and inverted organic optoelectronic devices," *Light Sci. Appl.*, vol. 4, 2015, Art. no. e273.
- [7] F. Guo, A. Karl, Q.-F. Xue, K. C. Tam, K. Forberich, and C. J. Brabec, "The fabrication of color-tunable organic light-emitting diode displays via solution processing," *Light Sci. Appl.*, vol. 6, 2017, Art. no. e17094.
- [8] S. Lim, D. Han, H. Kim, S. Lee, and S. Yoo, "Cu-based multilayer transparent electrodes: A low-cost alternative to ITO electrodes in organic solar cells," *Sol. Energy Mater. Sol. Cells*, vol. 101, pp. 170–175, 2012.
- [9] Y. G. Bi *et al.*, "Ultrathin and ultrasmooth Au films as transparent electrodes in ITO-free organic light-emitting devices," *Nanoscale*, vol. 8, no. 19, pp. 10010–10015, 2016.
- [10] O. Inganäs, "Avoiding indium," *Nature Photon.*, vol. 5, pp. 201–202, 2011.
- [11] M. Lee, Y. Ko, and Y. Jun, "Efficient fiber-shaped perovskite photovoltaics using silver nanowires as top electrode," *J. Mater. Chem. A*, vol. 3, no. 38, pp. 19310–19313, 2015.
- [12] M. Bissett, A. Barlow, C. Shearer, J. Quinton, and J. G. Shapter, "Comparison of carbon nanotube modified electrodes for photovoltaic devices," *Carbon*, vol. 50, no. 7, pp. 2431–2441, 2012.
- [13] C. Yu-Mo, L. Florent, S. Ishiang, and I. Ricardo, "A solution processed top emission OLED with transparent carbon nanotube electrodes," *Nanotechnology*, vol. 21, no. 13, 2010, Art. no. 134020.
- [14] Y. Chen *et al.*, "A two-step thermal annealing and HNO<sub>3</sub> doping treatment for graphene electrode and its application in small-molecule organic solar cells," *Org. Electron.*, vol. 38, pp. 35–41, 2016.
- [15] A. Kuruvila *et al.*, "Organic light emitting diodes with environmentally and thermally stable doped graphene electrodes," *J. Mater. Chem. C*, vol. 2, no. 34, pp. 6940–6945, 2014.
- [16] J.-Y. Hong, W. Kim, D. Choi, J. Kong, and H. S. Park, "Omnidirectionally stretchable and transparent graphene electrodes," *ACS Nano*, vol. 10, no. 10, pp. 9446–9455, 2016.
- [17] S. Kee *et al.*, "Controlling molecular ordering in aqueous conducting polymers using ionic liquids," *Adv. Mater.*, vol. 28, no. 39, pp. 8625–8631, 2016.
- [18] H.-Y. Xiang *et al.*, "Outcoupling-enhanced flexible organic light-emitting diodes on ameliorated plastic substrate with built-in indium–tin-oxide-free transparent electrode," *ACS Nano*, vol. 9, no. 7, pp. 7553–7562, 2015.
- [19] D. S. Ghosh, T. L. Chen, and V. Pruneri, "High figure-of-merit ultrathin metal transparent electrodes incorporating a conductive grid," *Appl. Phys. Lett.*, vol. 96, no. 4, 2010, Art. no. 041109.
- [20] J. Feng, Y. F. Liu, Y. G. Bi, and H. B. Sun, "Light manipulation in organic light-emitting devices by integrating micro/nano patterns," *Laser Photon. Rev.*, vol. 11, no. 2, 2017, Art. no. 1600145.
- [21] J. Zou, C. Z. Li, C. Y. Chang, H. L. Yip, and A. K. Y. Jen, "Interfacial engineering of ultrathin metal film transparent electrode for flexible organic photovoltaic cells," *Adv. Mater.*, vol. 26, no. 22, pp. 3618–3623, 2014.
- [22] D. Yin *et al.*, "Efficient and mechanically robust stretchable organic light-emitting devices by a laser-programmable buckling process," *Nature Commun.*, vol. 7, 2016, Art. no. 11573.
- [23] R. A. Hatton, M. R. Willis, M. A. Chesters, and D. Briggs, "A robust ultrathin, transparent gold electrode tailored for hole injection into organic light-emitting diodes," *J. Mater. Chem.*, vol. 13, no. 4, pp. 722–726, 2003.
- [24] R. Ding *et al.*, "Highly efficient three primary color organic single-crystal light-emitting devices with balanced carrier injection and transport," *Adv. Funct. Mater.*, vol. 27, no. 13, 2017, Art. no. 1604659.
- [25] Y.-F. Liu *et al.*, "Improved efficiency of indium–tin-oxide-free organic light-emitting devices using PEDOT:PSS/graphene oxide composite anode," *Org. Electron.*, vol. 26, pp. 81–85, 2015.
- [26] J. Kang, S. Atashin, S. H. Jayaram, and J. Z. Wen, "Frequency and temperature dependent electrochemical characteristics of carbon-based electrodes made of commercialized activated carbon, graphene and single-walled carbon nanotube," *Carbon*, vol. 111, pp. 338–349, 2017.

- [27] W. Kylberg *et al.*, "Woven electrodes for flexible organic photovoltaic cells," *Adv. Mater.*, vol. 23, no. 8, pp. 1015–1019, 2011.
- [28] K. Ellmer, "Past achievements and future challenges in the development of optically transparent electrodes," *Nature Photon.*, vol. 6, pp. 809–817, 2012.
- [29] G. Zhao *et al.*, "Stable ultrathin partially oxidized copper film electrode for highly efficient flexible solar cells," *Nature Commun.*, vol. 6, 2015, Art. no. 8830.
- [30] H. M. Stec, R. J. Williams, T. S. Jones, and R. A. Hatton, "Ultrathin transparent Au electrodes for organic photovoltaics fabricated using a mixed mono-molecular nucleation layer," *Adv. Funct. Mater.*, vol. 21, no. 9, pp. 1709–1716, 2011.
- [31] C. Cioarec, P. Melpignano, N. Gherardi, R. Clergereaux, and C. Villeneuve, "Ultrasmooth silver thin film electrodes with high polar liquid wettability for OLED microcavity application," *Langmuir*, vol. 27, no. 7, pp. 3611–3617, 2011.
- [32] M. G. Helander, Z. B. Wang, M. T. Greiner, Z. W. Liu, J. Qiu, and Z. H. Lu, "Oxidized gold thin films: An effective material for high-performance flexible organic optoelectronics," *Adv. Mater.*, vol. 22, no. 18, pp. 2037–2040, 2010.
- [33] N. Formica, D. S. Ghosh, A. Carrilero, T. L. Chen, R. E. Simpson, and V. Pruneri, "Ultrastable and atomically smooth ultrathin silver films grown on a copper seed layer," *ACS Appl. Mater. Interfaces*, vol. 5, no. 8, pp. 3048–3053, 2013.
- [34] S. Schubert, J. Meiss, L. Müller-Meskamp, and K. Leo, "Improvement of transparent metal top electrodes for organic solar cells by introducing a high surface energy seed layer," *Adv. Energy Mater.*, vol. 3, no. 4, pp. 438–443, 2013.
- [35] X.-L. Ou, M. Xu, J. Feng, and H.-B. Sun, "Flexible and efficient ITO-free semitransparent perovskite solar cells," *Sol. Energy Mater. Sol. Cells*, vol. 157, pp. 660–665, 2016.
- [36] W. Cao, Y. Zheng, Z. Li, E. Wrzesniewski, W. T. Hammond, and J. Xue, "Flexible organic solar cells using an oxide/metal/oxide trilayer as transparent electrode," *Org. Electron.*, vol. 13, no. 11, pp. 2221–2228, 2012.
- [37] K. Leosson, S. I. Arni, B. Agnarsson, A. Kossoy, S. Olafsson, and C. G. Malte, "Ultra-thin gold films on transparent polymers," *Nanophotonics*, vol. 1, pp. 3–11, 2013.
- [38] R. Ding *et al.*, "Fabrication and characterization of organic single crystal-based light-emitting devices with improved contact between the metallic electrodes and crystal," *Adv. Funct. Mater.*, vol. 24, no. 45, pp. 7085–7092, 2014.
- [39] D. Gu, C. Zhang, Y.-K. Wu, and L. J. Guo, "Ultrasmooth and thermally stable silver-based thin films with subnanometer roughness by aluminum doping," *ACS Nano*, vol. 8, no. 10, pp. 10343–10351, 2014.
- [40] R. Ma, J. Feng, D. Yin, and H.-B. Sun, "Highly efficient and mechanically robust stretchable polymer solar cells with random buckling," *Org. Electron.*, vol. 43, pp. 77–81, 2017.
- [41] H. Kang, S. Jung, S. Jeong, G. Kim, and K. Lee, "Polymer-metal hybrid transparent electrodes for flexible electronics," *Nature Commun.*, vol. 6, 2015, Art. no. 6503.
- [42] L. Vitos, A. V. Ruban, H. L. Skriver, and J. Kollár, "The surface energy of metals," *Surf. Sci.*, vol. 411, no. 1, pp. 186–202, 1998.
- [43] W. Chen, M. D. Thoreson, S. Ishii, A. V. Kildishev, and V. M. Shalaev, "Ultra-thin ultra-smooth and low-loss silver films on a germanium wetting layer," *Opt. Express*, vol. 18, no. 5, pp. 5124–5134, 2010.
- [44] R. G. Gordon, "Criteria for choosing transparent conductors," *MRS Bull.*, vol. 25, no. 8, pp. 52–57, 2000.
- [45] R. G. Gordon, "Preparation and properties of transparent conductors," *MRS Proc.*, vol. 426, 1996, Art. no. 419.